DNA Bending in Transcription Initiation†

Vladimir Tchernaenko,‡ Monika Radlinska,‡ Lucyna Lubkowska,§ Herbert R. Halvorson,‡ Mikhail Kashlev,§ and Leonard C. Lutter*,‡

Molecular Biology Section, Bone and Joint Center, Henry Ford Hospital, Detroit, Michigan 48202, and Molecular Mechanisms of Transcription Section, NCI Center for Cancer Research, Frederick Cancer Research and Development Center, Frederick, Maryland 27102

Received June 29, 2007; Revised Manuscript Received November 15, 2007

ABSTRACT: Electrophoretic mobility shift (bandshift) phasing analysis and rotational variant topological analysis were performed on initiation complexes formed on the bacteriophage lambda PR promoter. Both the open complex and an abortive complex containing a short RNA primer extending to +3 were characterized. The two methods were used to analyze a series of constructs containing tandemly repeated copies of the PR promoter, with the repeat length increased in single base pair increments to progressively change the rotational setting of adjacent copies. The phasing effect observed in bandshift analysis of open complexes formed on this set of constructs provided qualitative evidence for the presence of a bend. Subsequent rotational variant topological analysis confirmed this and quantified the overall bend angle in the open complex as well as in the +3 abortive complex: a bend of 49° ± 7° was measured for the open complex, while a bend of 47° ± 11° was measured for the +3 complex, i.e., the two bends are the same. However, the topological results are not consistent with extensive superhelical wrapping of DNA on either complex as has been proposed. The two complexes do differ in the size of the transcription bubble: the open complex contains a 10.4 ± 0.1 bp bubble, while that of the +3 complex is 12.2 ± 0.1 bp, a result consistent with "DNA scrunching" during the onset of transcription. A model for the overall path of the DNA in the open complex is presented that is consistent with the measured bend angle. Measurement of both bubble size and overall bend angle complements the results of crystal structures in providing an enhanced description of the solution structures of the intact initiation complexes.

Substantial progress has been achieved in structural analysis of the transcription machinery. Particularly impressive has been the advance in our understanding of the structure of the central component in transcription, RNA polymerase. Thus crystal structures have been determined that provide atomic detail of eukaryotic and prokaryotic RNA polymerases and their various complexes with DNA that model the enzyme open complex and elongation complex stages [reviewed recently in (*1*)]. No structure of the open promoter complex is available yet.

However, while these structures afford us unprecedented detail of the structure of RNA polymerase in several steps of transcription, the structures are at present incomplete. Thus only short segments of DNA are visualized in the crystallized complexes, and numerous questions remain concerning whether these structures represent functional states of the enzyme in solution. Moreover, crystallography necessarily describes a static structure that can be significantly affected by crystal packing, particularly with respect to the DNA component. Complexes of proteins with long DNA are particularly difficult to crystallize due to the flexible bulky nature of double-stranded DNA. One question that remains derives from the fact that there is as yet no description of an intact transcription bubble in crystal structures of either an open complex or an elongation complex. Although some crystals of elongation complex by RNA polymerase II contain transcription bubble, its structure is not resolved due to the high flexibility of DNA or a dynamic nature of protein−DNA interaction in the bubble area and in the duplex DNA located upstream from the bubble. Moreover, these structures are necessarily incomplete: the length of DNA (30 bp) visualized in cocrystals obtained to date is too short to reveal much about how the DNA may be wrapped on the surface of the polymerase.

A variety of approaches that study the structure of intact complexes in solution provide information that can complement the crystallographic results. Approaches such as nuclease protection assays indicate that polymerase interacts with an extensive stretch of DNA. Thus a number of studies of complexes at multiple prokaryotic promoters indicate that polymerase interacts with as much as 70−90 bp of DNA in the open complex [reviewed in (*2*)]. The fact that this length of DNA is considerably greater than the diameter of RNA polymerase led to the proposal that the DNA is wrapped on the surface of the polymerase in a manner similar to that of the nucleosome, with the most of the wrapping taking place with the upstream DNA [(*3*), reviewed in (*2*, *4*)]. Unfortunately there are no detailed structural studies available that would provide a comprehensive description for the overall path of such wrapping.

† This work was supported in part by grants from the National Institutes of Health (GM49988 and GM56216).

* Corresponding author. E-mail: llutter1@hfhs.org. Tel: 313-916-8681. Fax: 313-916-8064.

‡ Henry Ford Hospital.

§ Frederick Cancer Research and Development Center.

10.1021/bi7012883 CCC: $40.75
Published on Web 01/19/2008

One solution methodology that provided an important early clue about the wrapping that exists in the nucleosome is DNA topology. When a nucleosome binds to DNA and then that DNA is closed into a circle, the changes in DNA wrapping and duplex screw caused by nucleosome binding result in a change in the topological linking number of the circle relative to similarly treated bare DNA (*5*−*8*). The linking number quantifies the number of times one strand passes over the other in a DNA circle [reviewed in (*9*−*11*)]. A left-handed superhelical wrap will result in a linking number change (ΔL[1]) of −1, i.e., the linking number of the DNA circle will be reduced by one. In addition, unwinding the DNA duplex by one turn will also cause a change of −1. The linking number change is readily quantified by electrophoresis of the purified DNA in an agarose gel. This ability of the methodology to quantify changes in both wrapping and duplex screw contributed significantly to our understanding of nucleosome structure well before crystal structures (*12*, *13*) were available.

These advantages of the topological method led to its use in the study of the transcriptional open complex formed when RNA polymerase binds to DNA. The linking number change measured for polymerase bound to a specific promoter ranged from −1.0 to −1.7 (*14*−*17*). As reviewed in the accompanying paper (*18*), the change of −1.7 was interpreted as evidence for superhelical DNA wrapping [(*14*), also reviewed in (*4*)]. Thus chemical probe experiments (*19*−*22*) indicate that the open complex contains a bubble of about 12 bp, or unwinding of about one duplex turn, which corresponds to a linking number change of about −1. It was reasoned that the remaining −0.7 of the −1.7 measured reflects wrapping of 0.7 turn of left-handed superhelix on the complex surface (*14*). However, the results of other topological studies (*15*, *17*) do not lead to a prediction of wrapping; they find a linking number change closer to −1, which is near the value predicted for the bubble observed in the chemical probe studies. Thus in these cases there is no "excess" ΔL of −0.7 that can be assigned to left-handed superhelical wrapping. However, it is important to realize that the precision of the measurements in all of these studies is limited by the analysis of just one promoter copy [reviewed in (*18*)]. Moreover, the presence of additional promoters in the DNA circle used complicates the measurement in some of the studies. To address these uncertainties, this topological change is measured with a higher precision in the current study. This and the accompanying study (*18*) achieve this higher precision by (1) increasing the magnitude of the linking number change through the use of constructs containing 10 tandemly repeated promoter copies and (2) removal of the vector promoters from the circle so that the entire linking number change derives from the promoter of interest, i.e., the "background" linking number change is eliminated.

Bending of the DNA onto the polymerase into a wrap is indicated by the results of several other approaches to analyzing open complexes. Thus gel electrophoretic analysis of an open complex formed either at the end or in the middle of a linear DNA fragment (termed circular permutation) indicates that the DNA may be bent (*23*, *24*), although this method cannot distinguish the difference between bending and increased flexibility (*25*, *26*). Moreover, microscopy studies of complexes adsorbed to a surface observe a reduction in the contour length of DNA upon formation of an open complex, a result that has been interpreted to indicate extensive wrapping of DNA on the polymerase (*27*−*29*). However, the fact that the complex is adsorbed to a surface complicates the interpretation of such studies (*30*). Moreover, these methodologies for analyzing bending can provide only an approximation of the extent of the bend.

Rotational variant analysis is a topological method that can not only detect but also quantify DNA bending in both free DNA and DNA in a complex in solution (*31*−*35*). This method analyzes the linking number change induced by formation of a protein complex on a series of plasmid constructs in which the spacing of tandem protein binding sites is systematically varied in 1 bp increments. This method has been described in detail previously [the reader is directed in particular to Figure 1 in (*31*) as well as the review in (*32*)]. A brief explanation of the method follows: if we consider the example of a protein that bends the DNA of its binding site by 90°, binding the protein to a segment of DNA containing four tandem repeats of the site will cause the segment to form a square for some repeat length, which we will designate *C* bp. Binding the protein to a segment containing four $C + 1$ bp repeats will result in formation of a right-handed, squared superhelix. A DNA circle containing that segment will undergo a linking number change of +1 (relative to a similarly treated bare DNA) if the protein is bound in the presence of topoisomerase. Conversely, a circle containing four $C - 1$ bp repeats will form a left-handed superhelix, causing a linking number change of −1. This abrupt change from −1 to +1 as the repeat length progresses through *C* bp will progressively drop to 0 as further increases in the repeat length are made to $C + 5$ bp: this will form a zigzag structure that will cause no linking number change (it is not superhelical but planar). Further increments of single bp insertions will result in the left-handed superhelix at $C + 9$ bp repeat to give −1, at which point the abrupt change to +1 will repeat for $C + 11$ bp. A plot of linking number change versus repeat length will exhibit a "sawtooth" shape, with the amplitude of the sawtooth directly reflecting the number of repeats times the bend angle. The function relating linking number change to repeat length has been derived (*31*, *34*), and this is fitted to the data to obtain the bend angle. There are several advantages of this rotational variant method for measuring DNA bend angles. The measurement derives from first principles, requiring no comparison to standards of known bend angles such as has been attempted using gel electrophoretic methods. In addition, the method measures the bend angle of an active complex in solution. Rotational variant analysis has been applied to measurement of the bend angle induced by binding of the catabolite gene activator protein (*31*) as well as the intrinsic bend caused by the presence of an A-tract (*33*−*35*).

In the present study this rotational variant analysis is applied to both the open complex and the +3 abortive complex formed at the lambda bacteriophage PR promoter (λP_R). A circle containing ten tandem copies of the promoter is used to measure, with high precision, both the bend angle and the bubble size of the initiation complexes. No additional vector-derived promoters are present, thereby avoiding a complication of some earlier studies. The results provide

[1] Abbreviations: λP_R, the bacteriophage lambda PR promoter; ΔL, DNA topological linking number change.

insight into multiple aspects of the initiation process. The accompanying paper (*18*) describes a companion study that analyzes the transcription bubble in the open and abortive complexes.

MATERIALS AND METHODS

Plasmid Construction. A set of plasmids was generated in which each plasmid contains 5 tandem repeats of a fragment containing the λP_R promoter, with the repeat length increasing in 1−2 bp increments. The nomenclature is of the general form pPR*nnn*, with *nnn* designating the repeat length in base pairs. The methodologies for constructing these plasmids are variations of those described previously (*31*−*33*, *36*) and a brief description follows. A master PCR template was first generated by producing a fragment containing the λP_R promoter using PCR with primers LPR5 (5′GTCGCCCGAGCTAGATGCTGACTCATTGTCCCTATCACCGCAAGGGAT) and LPR3 (5′GGTGGCGGCCGCTCTAGAACTAGTGGATCCCTATTCCATACAACCTCC) in combination with *Alw*NI-cleaved plasmid pDW205 (kindly provided by Dr. R. Landick) as template. The 150 bp PCR product was then gel purified. This master template contains the λP_R promoter from −73 to +1 [significantly, it includes sequences to −60, which is the promoter sequence that has been used in the extensive characterization of λP_R complexes by footprinting studies from the Record laboratory (*3*, *37*−*41*)], followed by a sequence in which the first C is at C32 (see Figure 1A). The downstream end of the master template contains sequence complementary to that of the SKA set of rotational variant primers (*32*, *33*). This master template was then incubated in a series of PCR reactions containing primer LPR5 (which contains the appropriate *Ava*I sequence) and various SKA primers. This generated a set of fragments in which the distance between the *Ava*I sites varied between 145 bp and 157 bp. These fragments were cloned into T-vector (Promega), and the fragment containing the λP_R promoter was purified from a clone of each repeat length. Tandem repeats of each length fragment were then cloned into the *Ava*I site of pCLAV (*31*) using the initiator fragment procedure (*36*). This resulted in no more than trimer repeats for any of the fragments. Since much higher repeat numbers have been obtained with other sequences (*31*, *32*, *36*), it was surmised that the presence of large numbers of active λP_R promoters was detrimental to the cell. This was addressed by inserting a copy of the gene for the lambda repressor into pCLAV to generate pCLAR as the recipient plasmid for the oligomerization procedure. To construct pCLAR, a fragment containing the lambda repressor gene was excised from pDW205 by digestion with *Eco*RI, blunt-ending by Klenow DNA polymerase, and finally digesting with *Pst*I. This was cloned into pCLAV that had been digested with *Nde*I, blunt-ended, and cleaved with *Pst*I, to generate pCLAR. Use of pCLAR in the oligomer cloning procedure allowed the isolation of clones containing 5 repeats of λP_R. Clones containing 5 repeats and in single base increments were obtained for pPR143 through pPR157 (the last 3 digits designate the repeat length), with the exception of the 150 bp repeat length. To increase the number of repeats in a circle to 10 as well as to eliminate vector promoters, the *Apo*I/*Pst*I fragment containing the λP_R repeats was purified from each pPR*nnn* plasmid and ligated to generate a head-to-head dimer circle, designated cPR*nnn* (see Figure 1B). Finally, PCR mutagenesis was used to add a *Bpu*10I site between the *Sph*I and *Apo*I sites (see Figure 1B) so that the *Apo*I/*Pst*I dimer circle could be specifically nicked with *Nb.Bpu*10I to allow for closure of circles by ligation (see below). This was done for a subset of the of the pPR rotational variants, which were then termed pNPR*nnn* (pNLPR145, 146, 147, 148, 149, 151, 154, 156, and 157).

Bandshift Analysis. For Figure 2A, pPR157 (10 nM λP_R) was cleaved with *Sph*I and *Pst*I (see Figure 1B), after which it was incubated with RNA polymerase holoenzyme (20 nM) (Epicentre) for 15 min at 37 °C in 20 mM Tris, 50 mM NaCl, 10 mM $MgCl_2$, 1 mM dithiothreitol, 0.1 mM ethylenediaminetetraacetic acid (EDTA), 10% glycerol, and 0.1 mg/mL acetylated BSA. Samples were fractionated by electrophoresis in a 2% agarose in TAE buffer (40 mM Tris, 20 mM acetic acid, 1 mM EDTA, pH 8.0). For Figure 2B, each plasmid in the set of rotational variant plasmids was digested with *Apo*I, *Pst*I, and *Sml*I, after which the sample (5 nM λP_R) was incubated as with RNA polymerase (20 nM). Heparin (Sigma) was then added to 0.2 mg/mL and the sample was further incubated for 15 min at 37 °C. Finally, a sample of the digested bare DNA was added to serve as a bare DNA reference on the gel. All samples were then fractionated by electrophoresis in either a 0.6% or 3.0% agarose gel in TAE buffer. The relative mobility was calculated as the distance migrated by the band corresponding to the *Apo*I/*Pst*I fragment occupied by 5 polymerases divided by that of the bare fragment.

Topological Analysis. A typical binding reaction (20 μL) involved incubating the indicated amount of histidine-tagged RNA polymerase holoenzyme (*42*) with the appropriate *Nb.Bpu*10I-nicked DNA circle (2.6 nM, 26 nM λP_R) in 10 mM K-Hepes (pH 7.5), 150 mM NaCl, 0.1 mM EDTA, 0.033 mM NAD (Sigma), 10% glycerol, 0.1 mg/mL acetylated BSA (NEB), and 10 mM $MgCl_2$ for 10 min at 37 °C. For +3 abortive initiation complexes the oligoribonucleotide GCAUG (0.066 mM, Dharmacon) was added at this point and the incubation was continued for 10 min at 37 °C. Analysis of the radioactively labeled primer using size exclusion chromatography confirmed its stable binding to RNA polymerase λP_R (not shown). This was followed by the addition of *Escherichia coli* ligase (260 U/mL) and a further incubation of 20 min at 37°. Samples were then phenol extracted and ethanol precipitated, followed by fractionation by electrophoresis in an 0.6% agarose gel in the presence of 0.022 μg/mL ethidium bromide in TBE buffer (89 mM Tris-borate, 2 mM EDTA, pH 8.2). In some cases (e.g., Figure 3A) a short second dimension was run in the presence of 0.1 μg/mL ethidium bromide/TBE to separate the topoisomers from the nicked and linear species on the diagonal. From this point, data analysis was performed as described previously (*31*, *32*, *35*): the gel was stained in ethidium bromide and scanned (FMBio), after which the profile of each topoisomer distribution was obtained (MultiAnalyst, BioRad) and its center (corresponding to its mean linking number) was determined. The large linking number change in these complexes meant that resolution of the bare DNA distribution required different gel conditions (0.25 μg/mL chloroquine diphosphate rather than 0.022 μg/mL ethidium bromide. The linking number change was then measured by relating the topoisomer registers of the two samples via a series of "connector" samples. These were

generated by relaxation of bare DNA samples in the presence of increasing concentrations of chloroquine diphosphate, after which they were resolved on gels containing appropriate chloroquine concentrations (*33*). The difference between the two samples was then quantified by counting the topoisomer spots between the centers of the two distributions. This difference between the mean linking number of the sample ligated in the presence of polymerase and that ligated in its absence is the polymerase-induced linking number difference, i.e., $\Delta L = L_{+RP} - L_{bare}$. The equation relating ΔL to repeat length was fitted to the data set to obtain the bend angle (*31*−*33*, *35*), a process that is described briefly here. The linking number change contribution per interbend segment is composed of two components (further discussed in Results). One component, termed ΔL_{SH}, is the linking number change contribution per interbend segment that is due to the superhelix formed by successive bends, and varies with the repeat distance:

$$\Delta L_{SH} = (\arccos[\cos(B/2)\cos(\varphi_{av}/2)])/\pi - \varphi_{av}/2\pi$$

Here B is the bend angle induced by protein binding. φ_{av} is the dihedral angle between successive bends. It depends on binding site repeat length and the helical repeat length of the DNA duplex (DNA screw), and contains a term for torsional flexibility of the interbend DNA [see (*33*) for further discussion]. The second component, termed ΔL_I [also termed I in (*31*, *32*)], is the linking number change intrinsic to the monomer unit (e.g., the twist contribution in a single open complex that derives from unwinding the duplex during bubble formation), and as such does not vary with repeat length. The linking number change for a given construct is

$$\Delta L = L_{+RP} - L_{bare} = (n - 1)\Delta L_{SH} + (n)\Delta L_I$$

where n is the number of repeats in the construct. This is the general equation for a circle containing n contiguous repeats, which will contain $n - 1$ dihedral angles. In the special case here for cPR and cNPR (Figure 1), the repeats are arranged in two blocks of 5, which results in 10 repeats and 8 dihedral angles. Thus for these constructs, $\Delta L = (8)\Delta L_{SH} + (10)\Delta L_I$. This function was fitted to a plot of ΔL versus repeat length. Each data set (28 data points for the open complex, 30 data points for the +3 complex) was made up of results from at least three separate experiments. Fit results not discussed in results follow: The fit values for the DNA screws were similar (10.63 ± 0.02 for the open complex and 10.66 ± 0.02 for the +3 complex), but the values for the torsional flexibility of the repeat unit DNA [termed "σ" in (*32*, *35*) and defined as the standard deviation of the rotation per bp] differed: a value of 6.9 was obtained for the open complex, while 4.7 was obtained for the +3 complex. This is seen as a steeper slope in the plot of the +3 complex at the crossover point (about 149 bp repeat length), compared to that of the open complex [see (*31*, *32*, *35*) for discussion of this feature]. This indicates that the DNA of the repeat unit appears to be slightly stiffer in the +3 complex than in the open complex, but, as discussed previously (*35*), it is not a highly sensitive indicator of torsional stiffness in this system.

RNA polymerase complexes contain multiple bends [reviewed in (*2*, *4*, *43*)]. The rotational variant method measures the overall bend angle induced upon protein binding, i.e., the sum total of the composite bends. Indeed, the initial demonstration of the method measured the overall bend in solution of a complex of the catabolite gene activator protein (CAP) with its binding site (*31*). X-ray crystallographic analysis demonstrated that this overall bend is a composite of two sub-bends (*44*). A second rotational variant analysis of a composite bend analyzed the overall bend composed of 5 phased adenine tracts (A-tracts) that were approximately coplanar. Details of the relationship of the composite bends and the overall bend with respect to the rotational variant measurement have been discussed (*33*). To summarize, the method measures the overall bend, which is the sum total of the composite bends. If these bends are not coplanar, there can be a contribution to the linking number change intrinsic to the repeat unit, a quantity termed I in the CAP rotational variant study (*31*) and termed ΔL_I here (see above). The measurement in the CAP complex was $I = -0.067$ ($=\Delta L_I$). This small amount of negative ΔL_I is likely negative writhe ($-\Delta W_I$) deriving from the left-handed superhelical path of the two sub-bends observed in the crystal structure.

RESULTS

Generation of Rotational Variant Constructs of the λP_R Promoter. A series of DNA circles containing tandem repeats of the λP_R promoter was created in order to analyze the topological properties of transcription complex formation at the promoter. Features of these circles are shown in Figure 1. A fragment containing the λP_R promoter, and terminated by *Ava*I sites, was generated by PCR as described in Materials and Methods. An example containing a 157 repeat length between the *Ava*I sites is illustrated in Figure 1A. This *Ava*I-digested fragment was ligated into a vector at the identical *Ava*I site using the initiator fragment strategy (*36*) to generate a plasmid containing 5 head-to-tail copies of the fragment. Since the footprint of polymerase in an open complex covers ∼90 bp (*2*), repeat lengths in excess of this should be sufficient to avoid steric interference between adjacent complexes. On the other hand, the DNA repeat length needs to be short enough to ensure that the intervening free DNA has sufficient torsional stiffness to communicate the rotational positions of successive complexes. A previous study (*31*) demonstrated that ∼70−80 bp beyond the footprint is effective for this, so repeat lengths in the range of 140−160 bp were used for these polymerase studies. It was found that the host cell would tolerate no more than 5 copies of λP_R per plasmid (see Materials and Methods), so the *Apo*I/*Pst*I fragment was isolated from the plasmid and ligated to form a dimer circle (Figure 1B) containing 10 copies of λP_R (note that the head-to-head arrangement does not affect the topological measurements in this study, since a superhelix formed by one of the 5-repeat blocks retains its handedness, and therefore its linking number contribution, regardless of its orientation). Treatment of this circle with the nicking enzyme *Nb.Bpu*10I results in a circle with two nicks that can be ligated to achieve topological closure. Thus the linking number change induced by transcription complex formation can be measured by forming the complex on the nicked circle followed by ligation, after which the purified DNA can be compared with that ligated under identical conditions but in the absence of polymerase. In order to

FIGURE 1: Constructs. A. Sequence of the 157 bp repeat unit of the rotational variant plasmid pNPR157. The λP_R transcriptional start site is indicated, and upstream sequence is included to −73. The sequence of the primer SKA12 (*32*, *36*) used to generate this repeat lies at the right end, while primer used at the left end (LPR5) was specifically made for the λP_R sequence and was the same for the complete series of λP_R rotational variants (see Materials and Methods). B. A diagram of cNPR*nnn* (*nnn* refers to the number of bp in the repeat and ranges from 143 bp to 157 bp), a circle formed by head-to-head ligation of two copies of a fragment excised by *Pst*I and *Apo*I digestion of the plasmid pNPR*nnn*. The locations of the 10 repeats of the promoter fragment are shown, as are the *Sph*I and *Bpu*10I sites. The precursor to pNPR*nnn* is pPR*nnn*, which is nearly identical except that it lacks the *Nb.Bpu*10I site.

quantify the bend angle induced by transcription complex formation, a series of such circles, termed rotational variants, was generated (*33*) containing repeat lengths that increase in increments of 1−2 bp. Tandemly repeated copies are required for bend angle measurement by the rotational variant method (*32*), but the presence of 10 copies also amplifies the signal of a single promoter by 10-fold, permitting measurement of the linking number change per promoter with high precision. This, as well as the elimination of vector promoters, allows measurement of the linking number change per promoter to be performed with higher precision than was possible in earlier studies (*14*, *15*, *45*).

Bandshift Analysis of Open Complexes Formed on the Tandemly Repeated Copies of λP_R. Figure 2A shows the results of electrophoretic bandshift analysis (*46*) that was used to develop conditions for open complex formation, monitor occupancy of the tandemly repeated promoter copies, and ensure the absence of binding to nonpromoter sites in the sequence. The *Pst*I/*Sph*I fragment containing the five copies of λP_R was excised from pPR157 and incubated with RNA polymerase to form open complexes, followed by separation of the complexes by electrophoresis in an agarose gel. The left lane in Figure 2A shows the result of an incubation reaction that contained a subsaturating amount of polymerase. A series of 6 bands is visible. The highest mobility band exhibits the mobility of the bare DNA fragment and thus represents the unoccupied DNA fragment. The 5 bands of progressively lower mobility represent occupancy of 1 to 5 promoter copies, respectively. The right lane of Figure 2A shows a sample incubated with a higher amount of polymerase that results in the occupancy of all 5 sites. The single band demonstrates full occupancy of the 5 promoters with no nonspecific binding elsewhere in the DNA. This establishes conditions for specific saturation of the 5 λP_R copies.

Bandshift Analysis of the Rotational Variant Set. With binding conditions established for the open complex, the bandshift analysis was then applied to the full set of rotational variants to determine if evidence for polymerase-induced DNA bending could be detected. If a DNA site is bent, then a fragment that contains tandem repeats of that site will migrate more slowly in gel electrophoresis when the bends are in *cis* than when they are in *trans* [reviewed in (*47*, *48*)]. This "phasing effect" has been observed for intrinsic bends (*49*, *50*) as well as protein-induced bends (*25*, *51*, *52*) in complexes analyzed in acrylamide gels. Unfortunately, the complex containing 5 bound polymerases (∼3 MDa) does not enter acrylamide gels, although it does enter a 2% agarose gel (Figure 2A). However, it has been proposed that electrophoresis in agarose gels does not detect bending (*53*, *54*), although a subsequent study demonstrated that higher concentration agarose gels can detect curvature in bare DNA (*55*).

To evaluate these findings for the transcription complex, open complexes were formed under conditions of subsaturating polymerase on the *Apo*I/*Pst*I fragments (see Figure 1B) of each of the rotational variant. The samples were then fractionated by electrophoresis in 0.6% (Figure 2B, upper panel) and 3.0% (Figure 2B, lower panel) agarose gels. The 0.6% gel shows no detectable mobility variation with repeat length for any of the occupancy species. However, the 3.0% gel shows a marked variation in the mobility of the 5-occupied complex with repeat length. The mobility of the 5-occupied complex becomes progressively reduced as the repeat length increases from 143 bp, becoming maximally retarded at 148 and 149 bp. Then, as the repeat length is increased further, the mobility increases. A quantitative description of these results is shown in Figure 2C, where the relative mobility is plotted for each repeat length. These normalized data show the maximum reduction in mobility occurs at 148.5 bp. This is the repeat length at which successive polymerase-induced bends are expected to be in *cis* (*47*, *48*). The beginning of the reduction occurs initially at 145 bp and then recurs at about 155 bp, indicating a phase of about 10−11 bp. This is as expected for the insertion of individual base pairs of DNA duplex with a screw of 10−11 bp/turn. Accordingly, the zigzag structures, i.e., those in which successive bends are in *trans*, occur at repeat lengths of about 144 bp and 154 bp (see model structures at the bottom of Figure 2B). An independent indication of polymerase-induced bending is the distinct band splitting and broadening in the subsaturated species in the 3.0% gel. Thus the 5-occupied band is noticeably sharper than the bands of lower occupancy in the 3.0% gel (although not in the 0.6% gel), and numerous of the subsaturated bands are split into sub-bands (e.g., the splitting of the 3-occupied band in 157). Splitting of subsaturated species such as that seen in the 3.0% gel has been interpreted to indicate polymerase-induced

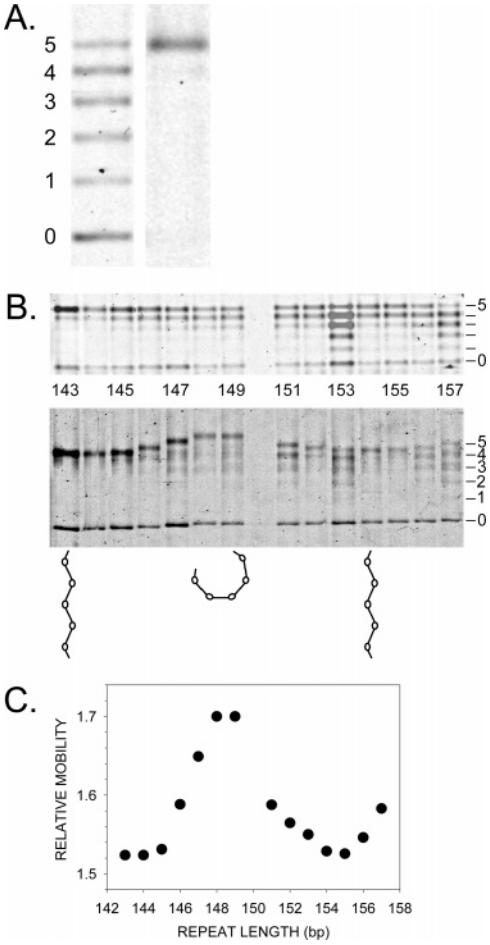

FIGURE 2: Bandshift analysis. A. Bandshift gel (2% agarose) of open complexes formed on a linear fragment excised by digestion of pPR157 with *Pst*I and *Sph*I (see Figure 1B). The sample in the lane on the left was incubated with a limiting amount of RNA polymerase in order to reveal the bandshift species corresponding to increasing occupancy by polymerase. The number of polymerases bound is indicated at the left of the lane. The sample in the channel at the right was incubated with a high level of polymerase, generating a single band occupied at all 5 sites. B. Bandshift gel analysis of rotational variant fragments. Rotational variant plasmids (pPR143 to pPR157) were each digested with *Apo*I and *Pst*I to excise a fragment containing the 5 λP_R binding sites (see Figure 1B). Each fragment was then incubated with a subsaturating amount of RNA polymerase to form open complexes, after which heparin was added along with a small amount of the original *Apo*I/*Pst*I fragment to serve as a bare DNA mobility marker. The samples were then fractionated by electrophoresis in agarose gels. The top panel shows a 0.6% agarose gel. At the side of the gel are indicated the mobilities of the bands corresponding to occupancy by 0 through 5 polymerases, while beneath is indicated the repeat length in bp. It can be seen that there is virtually no variation mobility of the 5-occupied band with repeat length. The lower panel shows the same samples fractionated in a 3.0% agarose gel. In contrast to the 0.6% gel above, the mobility of the 5-occupied band varies periodically with repeat length. The minimum mobility (148−149 bp) is predicted to represent the *cis* structure, drawn to approximate scale below the gel. The maximum mobilities occur at about half a duplex turn on either side (~143 bp and 154 bp) of the minimum mobility and are predicted to represent the *trans* structures. C. Plot of relative mobility versus repeat length for the 5-occupied band in the 3.0% agarose gel in Figure 2B. Relative mobility is the distance migrated by the 0-occupied band divided by that of the 5-occupied band. These results are representative of those from 7 independent experiments. Minimum mobility (corresponding to the maximally bent structure) occurs at 148.5 bp, while maximum mobility (corresponding to the extended, zigzag structures) occur about half duplex turn in either direction at ~143 and ~154 bp.

bending due to a "circular permutation" effect in multisite constructs that are partially occupied by polymerase (*24*).

This is to our knowledge the first demonstration by phasing analysis of DNA bending in the open complex. These findings extend those of circular permutation studies (*23*, *24*), which indicated that formation of open complex either bends the DNA or increases its flexibility. Phasing analysis such as that performed here does not suffer from this interpretation ambiguity (*25*, *56*), so the results here provide the first direct gel electrophoretic demonstration that the open complex bends the DNA rather than simply increases its flexibility. In addition to this, these results identify the repeat length that forms the *cis* structure and that which forms the *trans* structure. These are important preliminary results for the topological studies described below.

Measurement of the Bend Angle in a Transcription Initiation Complex by Topological Analysis. While the gel methods such as mobility anomaly described above are effective at demonstrating the presence of a bend or increased flexibility, they are not able to measure the actual bend angle (*47*). For this purpose, topological analysis of the rotational variant set of constructs (*31*, *32*) was used. In order to increase the sensitivity and specificity of the method, a head-to-head dimer circle (Figure 1B) was constructed from a repeat-containing fragment of each rotational variant plasmid (see Materials and Methods). The nickable, 157 bp repeat version of such a circle, cNPR157, contains 10 copies of λP_R arranged in two blocks of 5 tandemly repeated promoters per block (see diagram in Figure 1B). Figure 3A shows the topological effect of formation of open complexes on one such circle. *Nb.Bpu*10I-nicked cNPR149 was incubated with increasing amounts of RNA polymerase to form open complexes, after which DNA ligase was added to seal the nicks. The DNA was then extracted and fractionated by electrophoresis in an agarose gel containing sufficient ethidium bromide to resolve the closed circular DNA as a series of topoisomers. These are indicated by the dashes at the right side of the gel in Figure 3A. Lanes a−f show little difference in the centers of the respective topoisomer distributions, indicating that all samples are near the saturation point of the 10 λP_R copies in the circle. Lane g contains a "connector" sample (*33*) that permits measurement of the difference in linking number units between the center of the topoisomer distribution (mean linking number) of each sample and that of the sample ligated under identical conditions but in the absence of polymerase (analyzed on a separate gel; see Materials and Methods). This quantifies the polymerase-induced linking number difference ($\Delta L = L_{+RP} - L_{bare}$) for the open complex.

This difference is plotted in the graph on the right of Figure 3A. It confirms that the progressively higher concentrations of polymerase used in the gel in Figure 3A (left panel) generate a mean linking number that becomes slightly more negative with increasing polymerase, but it also shows that they are all dramatically more negative than that of the bare DNA. The value for ΔL at saturating polymerase concentration was determined by fitting a hyperbola function to the data (solid line, Figure 3A, right panel). The analysis yielded a value of -9.84 ± 0.05, which corresponds to -0.98/open complex. This is substantially less negative than the previously obtained value of -1.7 per open complex (*14*). This discrepancy will be discussed later.

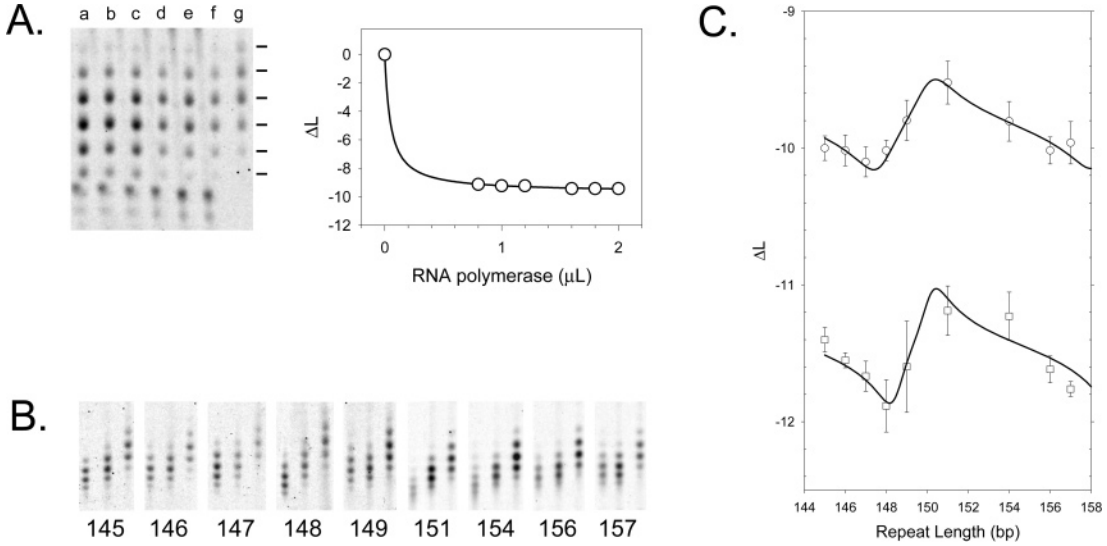

FIGURE 3: Topological analysis. A. Samples of *Nb.Bpu*10I-nicked cNPR149 (2.6 nM, 26 nM λP_R; see Figure 1B) were incubated at the following ratios of RNA polymerase to λP_R: a, 6.8; b, 8.5; c, 10.1; d, 13.5; e, 15.2; f, 16.9. Each was then incubated with DNA ligase to close the circle, after which the DNA was extracted and fractionated by two-dimensional electrophoresis in an agarose gel. The first dimension (top to bottom) contained 0.022 μg/mL ethidium bromide in TBE, while the second dimension (left to right) contained 0.1 μg/mL ethidium bromide in TBE and was run just long enough to separate the topoisomers from the nicked and linear fragments on the diagonal. Lane g contains the connector sample that relates the topoisomer linking number register here to that of DNA ligated in the absence of polymerase that was fractionated on a separate gel (see Materials and Methods). The mobilities of individual topoisomers are indicated at the right of the gel. The polymerase-induced linking number change (ΔL) was determined as the difference between the mean linking number of each DNA sample and that of DNA ligated without polymerase bound (see Materials and Methods). These values were plotted in the graph at the right. A hyperbola function was fitted to the data (solid line). This yields a value of $\Delta L = -9.84 \pm 0.05$ for the ten copy construct at saturation, or -0.984 ± 0.005/open complex. B. Topological analysis of polymerase complexes. Samples of *Nb.Bpu*10I-nicked cNPR*nnn* were incubated with a saturating concentration of RNA polymerase to form an open complex. A sample was then removed and further incubated with the oligonucleotide GCAUG to form a +3 complex. All samples were then incubated with DNA ligase, as described in part A above. The purified DNAs were then fractionated by one-dimensional electrophoresis in an agarose gel. There were three samples for each indicated repeat length. The left sample was the connector used to relate the register of the experimental samples to that of a sample ligated in the absence of polymerase. The middle sample was incubated with polymerase to form open complex. The right sample involved forming open complex followed by addition of the oligoribonucleotide GCAUG to form the +3 abortive complex. C. The polymerase-induced linking number change (ΔL) is plotted versus repeat length in the left panel. The symbols are open complex (circles) and +3 abortive complex (squares). The error bars represent the standard deviation of at least three independent experiments. The solid lines are the results of fitting the equation relating linking number change to repeat length (see Materials and Methods).

Having established conditions for measuring the linking number change of the open complex formation in the 10-site circle at saturation, a similar analysis was performed on a set of circles with other repeat lengths. The result of such an analysis is shown in Figure 3B. Each repeat length circle was incubated with an amount of polymerase sufficient to effectively saturate the 10 sites with open complexes. A sample was then removed and combined with the ribonucleotide GCAUG to form a complex containing an RNA oligonucleotide extending to +3. This corresponds to a +3 abortive complex [reviewed in (*2*)]. These two initiation complex versions of each circle were then incubated with DNA ligase to covalently close the circle, after which the extracted DNA was fractionated by electrophoresis in an agarose gel. There are 3 lanes in the gel (Figure 3B) for each repeat length circle. The left lane contains the connector used to relate the distribution to that of the same circle ligated in the absence of polymerase and analyzed on a separate gel (see above). The center lane contains the open complex sample, while the right lane contains the +3 abortive sample. It is immediately apparent from this gel that for all repeat lengths, the center of the topoisomer distribution of the +3 sample is about 1.5 topoisomer spots higher in the gel than that of the open complex. This means that the addition of GCAUG to the open complex has caused the mean linking number of the circle to decrease by about 1.5 linking number units in all repeat lengths.

A quantitative representation of the data is shown in Figure 3C. Here the initiation complex-induced linking number change ($\Delta L = L_{+RP} - L_{bare}$) for each repeat length was calculated by using the connector to relate the mean linking number of the sample to that of the sample ligated as bare DNA. The average ΔL values from multiple experiments are plotted versus repeat length in Figure 3C. A complete description of this type of plot is presented elsewhere [see especially Figure 1 of (*31*) and a review in (*32*)]. To explain briefly, if the repeat unit is bent upon binding polymerase, the systematic increase in the repeat length will generate a family of superhelices with progressively changing pitch. This produces a plot that periodically exhibits an abrupt rise, followed by a more gradual decrease, i.e., a plot that exhibits a "sawtooth" appearance (for reference, a complex in which the DNA remains straight after binding will generate no superhelices and a straight horizontal plot will result). The center of the abrupt rise is the repeat length at which the hand of the superhelix changes from left to right (the "crossover point"), while the amplitude of the plot reflects the magnitude of the bend the angle. This sawtooth appearance is observed in data Figure 3C for both the open complex (circles) and the +3 abortive complex (squares) and demonstrates that both complexes bend the promoter DNA upon formation. The center of the relatively abrupt rise, i.e., the superhelix crossover point, occurs at a repeat length of about 149 bp for both the complexes, and is the repeat length at

which the successive bends are in *cis*. This in turn agrees well with the finding of the open complex bandshift analysis in Figure 2C that the *cis* repeat length is between 148 and 149 bp. Thus both the bandshift analysis and the topological analysis of the rotational variants indicate that the open complex bends the promoter DNA when it forms, and the rotational variant analysis further demonstrates that the DNA is bent in the +3 abortive complex as well.

The magnitudes of the two bends as well as other structural parameters were quantified by fitting the equation relating ΔL and repeat length to the two sets of data [see Materials and Methods; (*31*−*33*, *35*)]. These fits are the solid lines through the two respective data sets in Figure 3C. The bend angle of the open complex obtained from the fit was 49° ± 7° while that obtained for the +3 complex was 47° ± 11°, i.e., the bend angles are the same for the two complexes.

The analysis of the data in Figure 3C also provides a measurement of the transcription bubble. As described above and elsewhere (*31*−*33*, *35*), the value of the bend angle derives from the component of the linking number change that varies with repeat length. We term this variable portion of the linking number change ΔL_{SH} (for a single interbend segment, see Materials and Methods) to reflect its origin in the progressively changing superhelices that result from changing the repeat length when the DNA is bent. This is the portion that generates the sawtooth shape of the curve, the amplitude of which is proportional to the bend angle. The remainder of the linking number change is a part that does not change with repeat length, which we term ΔL_I here (for a single repeat, see Materials and Methods). The total linking number change for a given repeat length is the sum of these repeat-length-dependent and -independent components. It follows that the total linking number change equals the repeat-length-independent component when the repeat-length-dependent component equals 0. This is the case when the bending is in a plane (as opposed to a superhelix) because planar bending does not contribute a linking number change (*9*). This occurs at the crossover point (coplanar bends in *cis*, at 148.9 bp for RPo), and half a duplex turn away when the bend are in the zigzag form (coplanar bends in trans, at 154.2 for RPo). ΔL_I is the linking number change intrinsic to the individual repeat unit, and in the case of the open complex its predominant cause is the twist change that occurs with unwinding of the duplex upon transcription bubble formation [see (*18*) for a detailed discussion]. ΔL_I determines the vertical displacement of the respective curves in Figure 3C. Note that for these open and abortive complexes, the major component of the linking number change is ΔL_I. This can be seen directly in Figure 3C: the downward displacement of the curve (representing ΔL_I) for the open complex is about −10, while the amplitude of the variation of the curve (representing ΔL_{SH}) is only about 0.5. This means that the contribution of the bubble to the linking number change is always much greater than that of the bend, which means that studies of the bubble (*18*) can be performed with any of these λP_R rotational variant constructs.

The distinct offset of the two respective topoisomer distributions for each repeat length in the original data (Figure 3B, discussed above) and the vertical separation of the plots of the two complexes in Figure 3C are due to the fact that the open and +3 abortive complexes have different values of ΔL_I, and thus different sizes of bubble. For open complex, $n\Delta L_I = -9.83 \pm 0.06$ (standard deviation from the fit), which calculates to -0.983 ± 0.006 per complex and corresponds to a transcription bubble of 10.4 ± 0.1 bp. This agrees reasonably well with estimates from alternative methods reported in the literature (see below). In contrast, the +3 abortive complex value of $n\Delta L_I = -11.45 \pm 0.13$ calculates to -1.145 ± 0.013 per complex, which corresponds to a transcription bubble of 12.2 ± 0.1 bp. This indicates that the addition of the RNA oligonucleotide to +3 extends the 3′ end of the bubble while the 5′ end remains stationary, resulting in a net expansion of the bubble. These and other features will be discussed further below.

DISCUSSION

The results in this study are relevant to several aspects of the solution structure of the transcription initiation complex: an overall DNA bend, DNA wrapping on the polymerase surface, and DNA bubble formation. These will be discussed in turn below.

An overall DNA bend in the transcription initiation complex was detected using two methods: phasing analysis of the open complex bandshift, and rotational variant analysis of both the open complex and the +3 complex. Bending in the open complex has been suggested previously using version of circular permutation analysis of bandshifts in acrylamide gels (*23*, *24*, *57*, *58*), but this method is unable to distinguish between bending and increased flexibility of DNA induced by complex formation angle (*47*).

Our bandshift phasing analysis (Figure 2B) resolves this ambiguity: the phase-dependent variation in electrophoretic mobility demonstrates that there is a bend in the open complex. None of the gel electrophoretic methods can reliably determine the bend angle (*33*, *47*), but this phasing analysis provides important preliminary information for the method that is able to measure bend magnitude, rotational variant analysis. Specifically, the bandshift phasing analysis determines the repeat length at which successive open complex bends are in *cis*. This is the repeat length for the crossover point from left-handed to right-handed superhelix in the rotational variant analysis. The fact that both methods independently identify that same repeat length (148−149 bp) for this point strongly supports the validity of each method for detecting a bend in the open complex. Moreover, the topological analysis extends this to demonstrate a bend in the +3 complex as well.

As described above, a unique strength of the rotational variant method is its ability to quantify the bend angle from first principles, avoiding the need for reference to bend standards, and to do this for active complexes in solution (*31*, *32*). This method measures an open complex bend of 49° ± 7°, while that measured in the +3 abortive complex is 47° ± 11°. Thus the two complexes bend DNA to the same extent, although they differ in bubble size, a finding that is discussed in detail in the accompanying paper (*18*). The equivalence in bend angle for the open and abortive complexes indicates that the overall path of the DNA changes little when transcription begins, with the primary change being DNA "scrunching" (*18*). The measurement in the +3 complex is to our knowledge the first detection and direct measurement of the bend angle in an abortive initiation complex. The bend angle obtained for the open complex

agrees with that of another solution method which used electrooptics to measure a bend of 45° ± 5° (*30*).

The possibility of DNA wrapping on the surface of polymerase, initially indicated by the footprinting data (*2*), means that the total bending could be considerably greater (*27*) than that measured by the rotational variant method here. Thus the 49° bend measured could reflect a bend of $N \times (360°) + 49°$ or $N \times (360°) - 49°$ (where N is the integer number of superhelical wraps). However, this ambiguity can be resolved by considering ΔL_I. As discussed above, the bend angle value derives from ΔL_{SH}, while the linking number change inherent to the individual repeat is ΔL_I. Overall, ΔL_I reflects changes in DNA wrapping (a change in topological writhe, or ΔW_I) and duplex screw [a change in topological twist, or ΔT_I, with $\Delta L_I = \Delta T_I + \Delta W_I$, see (*31*, *32*)] upon protein binding. In the case of polymerase, it is the sum of the change due to superhelical wrapping on its surface (ΔW_I) and the change in duplex screw due to unwinding to form the transcription bubble (ΔT_I).

As discussed in the introduction, chemical probe experiments indicate that about 1 turn of duplex is unwound during the formation of the transcription bubble (*19*−*22*). This would be expected to result in $\Delta L_I = \Delta T_I = -1$ in the open complex, a value that is essentially the same as the value of $\Delta L_I = -0.983 \pm 0.006$ measured here for the open complex. This indicates that there is no extensive superhelical wrapping (since $\Delta W_I = 0$) induced upon open complex formation. If the 49° bend observed here actually represented a superhelical wrap that is 49° short of a full turn [e.g., Figure 8 in (*27*)], i.e., 360° − 49°, then this would contribute a writhe change of about 0.9 [=(360 − 49)/360]. This would be negative if the superhelical wrap were left handed, in which case $\Delta L_I = \Delta T_I + \Delta W_I = (-1) + (-0.9) = -1.9$. This would be positive if the superhelical wrap were right handed, thus $\Delta L_I = \Delta T_I + \Delta W_I = (-1) + (+0.9) = -0.1$. The measured value of value of $\Delta L_I = -0.983 \pm 0.006$ agrees with neither, indicating that the DNA does not wrap extensively in a superhelix on the surface of the polymerase. Thus the value measured for ΔL_I eliminates simple models of nucleosome-like, superhelical wrapped DNA [e.g., as proposed in Figure 8 in (*27*)]. The explanation for the substantial evidence for wrapping in the open complex [reviewed in (*4*)] must be that most of the wrapping is not superhelical [see also a detailed discussion in (*18*) on this point relative to earlier topological measurements of the open complex (*14*)].

Crystal structures indicate a bend considerably greater than the ∼50° bend that we measure here in the open complex. While there are no crystal structures of an intact open complex, crystal structures of elongation complexes exhibit a 90° bend into the polymerase in the region of the active site (*59*−*61*). If this bend is also present in the open complex, a possible path of the complex DNA that incorporates our finding of a ∼50° bend is presented in Figure 4. Here the 90° bend can be seen at the leading end of the transcription bubble. The DNA upstream of the bubble contacts the 3/4 domains of the σ subunit, at which point the DNA bends back to contact the C-terminal domains of the two α subunits (*29*, *62*−*64*). This results in an overall bend of 50° as measured in this study, but, as diagrammed, the bend is in the opposite direction from the 90° bend at the active site. This is of course a simplified diagram, e.g., the two DNA bends are shown to be in one plane, but this is only for ease of demonstration and is not meant to imply that they are necessarily planar in the actual structure. However, it demonstrates how the 90° bend in the active site portion of the DNA observed in the crystal structure may be just one of multiple bends that result in the overall bend of 50° measured here. It will of course be of interest to determine the overall path of the open complex DNA as well as how that path may change upon conversion to an elongation complex.

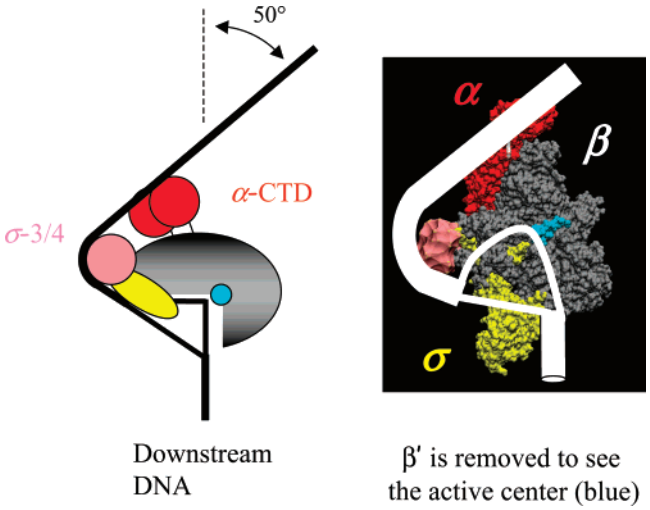

FIGURE 4: Possible internal arrangement of open complex DNA. On the left is shown a schematic diagram of the open complex, including the C-terminal domains of the two α subunits (red), domains 3 and 4 of the σ subunit (pink), the remainder of the σ subunit (yellow), the active center (blue) the remainder of the polymerase (gray) and the DNA (black) including the transcription bubble. The path of the DNA results in a ∼50° overall bend as measured in this study. On the right is shown this DNA path superimposed on the holoenzyme structure (*65*) from which has been removed the β' subunit to allow visualization of the active center.

ACKNOWLEDGMENT

We would like to thank Olga Shabalin for excellent technical assistance. The contents of this publication do not necessarily reveal the views or policies of the Department of Health and Human Services, nor does mention of trade names, commercial product, or organizations imply endorsement by the U.S. Government.

REFERENCES

1. Boeger, H., Bushnell, D. A., Davis, R., Griesenbeck, J., Lorch, Y., Strattan, J. S., Westover, K. D., and Kornberg, R. D. (2005) Structural basis of eukaryotic gene transcription, *FEBS Lett. 579*, 899−903.
2. Record, M. T. Jr., Reznikoff, W. S., Craig, M. L., McQuade, K. L., and Schlax, P. J. (1996) *Escherichia coli* RNA polymerase ($E\sigma^{70}$), promoters, and the kinetics of the steps of transcirption initiation, in *Escherichia coli and Salmonella typhimurium: Cellular and Molecular Biology* (Neidhardt, F. C., Ed.) pp 792−821, ASM Press, Washington, D.C.
3. Craig, M. L., Suh, W. C., and Record, M. T., Jr. (1995) HO• and DNase I probing of $E\sigma^{70}$ RNA polymerase−λP_R promoter open complexes: Mg^{2+} binding and its structural consequences at the transcription start site, *Biochemistry 34*, 15624−15632.
4. Coulombe, B., and Burton, Z. F. (1999) DNA bending and wrapping around RNA polymerase: a "revolutionary" model describing transcriptional mechanisms, *Microbiol. Mol. Biol. Rev. (Washington, DC) 63*, 457−478.
5. Germond, J. E., Hirt, B., Oudet, P., Gross-Bellard, M., and Chambon, P. (1975) Folding of the DNA double helix in

chromatin-like structures from simian virus 40, *Proc. Natl. Acad. Sci. U.S.A. 72*, 1843−1847.
6. Keller, W. (1975) Determination of the number of superhelical turns in simian virus 40 DNA by gel electrophoresis, *Proc. Natl. Acad. Sci. U.S.A. 72*, 4876−4880.
7. Lutter, L. C., Judis, L., and Paretti, R. F. (1992) The effects of histone acetylation on chromatin topology in vivo, *Mol. Cell. Biol. 12*, 5004−5014.
8. Drabik, C. E., Nicita, C. A., and Lutter, L. C. (1997) Measurement of the linking number change in transcribing chromatin, *J. Mol. Biol. 267*, 794−806.
9. Crick, F. H. (1976) Linking numbers and nucleosomes, *Proc. Natl. Acad. Sci. U.S.A. 73*, 2639−2643.
10. Bates, A. D. and Maxwell, A. (2005) *DNA Topology*, IRL Press at Oxford University Press, Oxford.
11. Sinden, R. R. (1994) *DNA Structure and Function*, Academic Press, San Diego, New York.
12. Finch, J. T., Lutter, L. C., Rhodes, D., Brown, R. S., Rushton, B., Levitt, M., and Klug, A. (1977) Structure of nucleosome core particles of chromatin, *Nature 269*, 29−36.
13. Richmond, T. J., and Davey, C. A. (2003) The structure of DNA in the nucleosome core, *Nature 423*, 145−150.
14. Amouyal, M., and Buc, H. (1987) Topological unwinding of strong and weak promoters by RNA polymerase. A comparison between the lac wild-type and the UV5 sites of Escherichia coli, *J. Mol. Biol. 195*, 795−808.
15. Su, T. T., and McClure, W. R. (1994) Selective binding of Escherichia coli RNA polymerase to topoisomers of minicircles carrying the TAC16 and TAC17 promoters, *J. Biol. Chem. 269*, 13511−13521.
16. Buc, H., and McClure, W. R. (1985) Kinetics of open complex formation between Escherichia coli RNA polymerase and the lac UV5 promoter. evidence for a sequential mechanism involving three steps, *Biochemistry 24*, 2712−2723.
17. Bertrand-Burggraf, E., Schnarr, M., Lefevre, J. F., and Daune, M. (1984) Effect of superhelicity on the transcription from the tet promoter of pBR322. abortive initiation and unwinding experiments, *Nucleic Acids Res. 12*, 7741−7752.
18. Tchernaenko, V., Halvorson, H. R., Kashlev, M., and Lutter, L. C. (2008) DNA bubble formation in transcription initiation, *Biochemistry 47*, 1871−1884.
19. Siebenlist, U. (1979) RNA polymerase unwinds an 11-base pair segment of a phage T7 promoter, *Nature 279*, 651−652.
20. Siebenlist, U., Simpson, R. B., and Gilbert, W. (1980) E. coli RNA polymerase interacts homologously with two different promoters, *Cell 20*, 269−281.
21. Spassky, A., Kirkegaard, K., and Buc, H. (1985) Changes in the DNA structure of the lac UV5 promoter during formation of an open complex with Escherichia coli RNA polymerase, *Biochemistry 24*, 2723−2731.
22. Kirkegaard, K., Buc, H., Spassky, A., and Wang, J. C. (1983) Mapping of single-stranded regions in duplex DNA at the sequence level: single-strand-specific cytosine methylation in RNA polymerase-promoter complexes, *Proc. Natl. Acad. Sci. U.S.A. 80*, 2544−2548.
23. Kuhnke, G., Theres, C., Fritz, H. J., and Ehring, R. (1989) RNA polymerase and gal repressor bind simultaneously and with DNA bending to the control region of the Escherichia coli galactose operon, *EMBO J. 8*, 1247−1255.
24. Heumann, H., Ricchetti, M., and Werel, W. (1988) DNA-dependent RNA polymerase of Escherichia coli induces bending or an increased flexibility of DNA by specific complex formation, *EMBO J. 7*, 4379−4381.
25. Zinkel, S. S., and Crothers, D. M. (1987) DNA bend direction by phase sensitive detection, *Nature 328*, 178−181.
26. Kerppola, T. K., and Curran, T. (1991) Fos-Jun heterodimers and Jun homodimers bend DNA in opposite orientations: implications for transcription factor cooperativity, *Cell 66*, 317−326.
27. Rivetti, C., Guthold, M., and Bustamante, C. (1999) Wrapping of DNA around the E. coli RNA polymerase open promoter complex, *EMBO J. 18*, 4464−4475.
28. Rees, W. A., Keller, R. W., Vesenka, J. P., Yang, G., and Bustamante, C. (1993) Evidence of DNA bending in transcription complexes imaged by scanning force microscopy, *Science 260*, 1646−1649.
29. Cellai, S., Mangiarotti, L., Vannini, N., Naryshkin, N., Kortkhonjia, E., Ebright, R. H., and Rivetti, C. (2007) Upstream promoter sequences and alphaCTD mediate stable DNA wrapping within the RNA polymerase-promoter open complex, *EMBO Rep. 8*, 271−278.
30. Meyer-Almes, F. J., Heumann, H., and Porschke, D. (1994) The structure of the RNA polymerase-promoter complex. DNA-bending-angle by quantitative electrooptics, *J. Mol. Biol. 236*, 1−6.
31. Lutter, L. C., Halvorson, H. R., and Calladine, C. R. (1996) Topological measurement of protein-induced DNA bend angles, *J. Mol. Biol. 261*, 620−633.
32. Lutter, L. C., Drabik, C. E., and Halvorson, H. R. (2000) Use of topology to measure protein-induced DNA bend and unwinding angles, in *Protein−DNA Interactions: A Practical Approach* (Travers, A. A. and Buckle, M., Eds.) pp 47−64, Oxford University Press, Oxford.
33. Tchernaenko, V., Radlinska, M., Drabik, C. E., Bujnicki, J. M., Halvorson, H. R., and Lutter, L. C. (2003) Topological measurement of the A-tract bend angle: comparison of bent and straightened states, *J. Mol. Biol. 326*, 737−749.
34. Tchernaenko, V., Halvorson, H. R., and Lutter, L. C. (2003) Topological measurement of the A-tract bend angle: variation of duplex winding, *J. Mol. Biol. 326*, 751−760.
35. Tchernaenko, V., Halvorson, H. R., and Lutter, L. C. (2004) Topological measurement of an A-tract bend angle: effect of magnesium, *J. Mol. Biol. 341*, 55−63.
36. Radlinska, M., Drabik, C. E., Tong, W. S., and Lutter, L. C. (2001) Generating tandem repeats by cloning with double initiator fragments, *BioTechniques 31*, 340−347.
37. Craig, M. L., Tsodikov, O. V., McQuade, K. L., Schlax, P. E. Jr., Capp, M. W., Saecker, R. M., and Record, M. T. Jr. (1998) DNA footprints of the two kinetically significant intermediates in formation of an RNA polymerase-promoter open complex: evidence that interactions with start site and downstream DNA induce sequential conformational changes in polymerase and DNA, *J. Mol. Biol. 283*, 741−756.
38. Tsodikov, O. V., Craig, M. L., Saecker, R. M., and Record, M. T. Jr. (1998) Quantitative analysis of multiple-hit footprinting studies to characterize DNA conformational changes in protein-DNA complexes: application to DNA opening by Esigma70 RNA polymerase, *J. Mol. Biol. 283*, 757−769.
39. Davis, C. A., Capp, M. W., Record, M. T. Jr., and Saecker, R. M. (2005) The effects of upstream DNA on open complex formation by Escherichia coli RNA polymerase, *Proc. Natl. Acad. Sci. U.S.A. 102*, 285−290.
40. Kontur, W. S., Saecker, R. M., Davis, C. A., Capp, M. W., and Record, M. T. Jr. (2006) Solute probes of conformational changes in open complex (RPo) formation by Escherichia coli RNA polymerase at the lambdaPR promoter: evidence for unmasking of the active site in the isomerization step and for large-scale coupled folding in the subsequent conversion to RPo, *Biochemistry 45*, 2161−2177.
41. Davis, C. A., Bingman, C. A., Landick, R., Record, M. T. Jr., and Saecker, R. M. (2007) Real-time footprinting of DNA in the first kinetically significant intermediate in open complex formation by Escherichia coli RNA polymerase, *Proc. Natl. Acad. Sci. U.S.A. 104*, 7833−7838.
42. Komissarova, N., and Kashlev, M. (1997) Transcriptional arrest: Escherichia coli RNA polymerase translocates backward, leaving the 3′ end of the RNA intact and extruded, *Proc. Natl. Acad. Sci. U.S.A. 94*, 1755−1760.
43. Murakami, K. S., and Darst, S. A. (2003) Bacterial RNA polymerases: the wholo story, *Curr. Opin. Struct. Biol. 13*, 31−39.
44. Schultz, S. C., Shields, G. C., and Steitz, T. A. (1991) Crystal structure of a CAP-DNA complex: the DNA is bent by 90 degrees, *Science 253*, 1001−1007.
45. Gamper, H. B., and Hearst, J. E. (1982) A topological model for transcription based on unwinding angle analysis of E. coli RNA polymerase binary, initiation and ternary complexes, *Cell 29*, 81−90.
46. Pindolia, K., and Lutter, L. C. (2005) Purification and characterization of the simian virus 40 transcription complex, *J. Mol. Biol. 349*, 922−932.
47. Hagerman, P. J. (1990) Sequence-directed curvature of DNA, *Annu. Rev. Biochem. 59*, 755−781.
48. Crothers, D. M., Haran, T. E., and Nadeau, J. G. (1990) Intrinsically bent DNA, *J. Biol. Chem. 265*, 7093−7096.
49. Hagerman, P. J. (1985) Sequence dependence of the curvature of DNA: a test of the phasing hypothesis, *Biochemistry 24*, 7033−7037.

50. Koo, H. S., Wu, H. M., and Crothers, D. M. (1986) DNA bending at adenine-thymine tracts, *Nature 320*, 501−506.

51. Salvo, J. J., and Grindley, N. D. F. (1987) Helical phasing between DNA bends and the determination of bend direction, *Nucleic Acids Res. 15*, 9771−9779.

52. Kerppola, T. K., and Curran, T. (1991) DNA bending by Fos and Jun: the flexible hinge model, *Science 254*, 1210−1214.

53. Marini, J. C., Levene, S. D., Crothers, D. M., and Englund, P. T. (1982) Bent helical structure in kinetoplast DNA, *Proc. Natl. Acad. Sci. U.S.A. 79*, 7664−7668.

54. Anderson, J. N. (1986) Detection, sequence patterns and function of unusual DNA structures, *Nucleic Acids Res. 14*, 8513−8533.

55. Calladine, C. R., Collis, C. M., Drew, H. R., and Mott, M. R. (1991) A study of electrophoretic mobility of DNA in agarose and polyacrylamide gels, *J. Mol. Biol. 221*, 981−1005.

56. Kerppola, T. K. (1997) Comparison of DNA bending by Fos-Jun and phased A tracts by multifactorial phasing analysis, *Biochemistry 36*, 10872−10884.

57. Kuhnke, G., Fritz, H. J., and Ehring, R. (1987) Unusual properties of promoter-up mutations in the Escherichia coli galactose operon and evidence suggesting RNA polymerase-induced DNA bending, *EMBO J. 6*, 507−513.

58. Heumann, H., Metzger, W., and Niehorster, M. (1986) Visualization of intermediary transcription states in the complex between escherichia coli DNA-dependent RNA polymerases and a promoter-carrying DNA fragment using the gel retardation method, *Eur. J. Biochem. 158*, 575−579.

59. Gnatt, A. L., Cramer, P., Fu, J., Bushnell, D. A., and Kornberg, R. D. (2001) Structural basis of transcription: an RNA polymerase II elongation complex at 3.3 A resolution, *Science 292*, 1876−1882.

60. Vassylyev, D. G., Vassylyeva, M. N., Zhang, J., Palangat, M., Artsimovitch, I., and Landick, R. (2007) Structural basis for substrate loading in bacterial RNA polymerase, *Nature*, advanced online publication. doi: 10.1038/nature05931.

61. Vassylyev, D. G., Vassylyeva, M. N., Perederina, A., Tahirov, T. H., and Artsimovitch, I. (2007) Structural basis for transcription elongation by bacterial RNA polymerase, *Nature*, advanced online publication. doi:10.1038/nature05932.

62. Chen, H., Tang, H., and Ebright, R. H. (2003) Functional interaction between RNA polymerase alpha subunit C-terminal domain and sigma70 in UP-element- and activator-dependent transcription, *Mol. Cell 11*, 1621−1633.

63. Ross, W., Aiyar, S. E., Salomon, J., and Gourse, R. L. (1998) Escherichia coli promoters with UP elements of different strengths: modular structure of bacterial promoters, *J. Bacteriol. 180*, 5375−5383.

64. Minakhin, L., and Severinov, K. (2003) On the role of the Escherichia coli RNA polymerase sigma 70 region 4.2 and alpha-subunit C-terminal domains in promoter complex formation on the extended -10 galP1 promoter, *J. Biol. Chem. 278*, 29710−29718.

65. Vassylyev, D. G., Sekine, S., Laptenko, O., Lee, J., Vassylyeva, M. N., Borukhov, S., and Yokoyama, S. (2002) Crystal structure of a bacterial RNA polymerase holoenzyme at 2.6 A resolution, *Nature 417*, 712−719.

BI7012883